SOLAR CYCLE VARIATIONS OF LARGE SCALE FLOWS IN THE SUN

Sarbani Basu
Institute for Advanced Study, Olden Lane, Princeton NJ 08540, U. S. A. and Astronomy Department, Yale University, P.O. Box 208101 New Haven, CT 06520-8101 USA

H. M. Antia
Tata Institute of Fundamental Research, Homi Bhabha Road, Mumbai 400005, India

February 5, 2008

Abstract. Using data from the Michelson Doppler Imager (MDI) instrument on board the Solar and Heliospheric Observatory (SOHO), we study the large-scale velocity fields in the outer part of the solar convection zone using the ring diagram technique. We use observations from four different times to study possible temporal variations in flow velocity. We find definite changes in both the zonal and meridional components of the flows. The amplitude of the zonal flow appears to increase with solar activity and the flow pattern also shifts towards lower latitude with time.

Keywords: Sun: General – Sun: Interior – Sun: Oscillations – Sun: rotation

1. Introduction

Ring diagram analysis has been extensively used to infer horizontal flows in the outer part of the solar convection zone (Hill 1988; Patrón et al. 1997; Basu, Antia and Tripathy 1999). This technique is based on the study of three-dimensional power spectra of solar p-modes on a part of the solar surface, and can be used to study the variation in flow velocity with latitude, longitude and time. The latitudinal variation of flow velocities in both the rotational and meridional component has been extensively studied (Schou and Bogart 1998; Basu et al. 1999; Gonzalez Hernandez et al. 1999) and there is a reasonable agreement between results obtained by different workers. There is some indication that the flow velocity also changes with longitude and time (Patrón et al. 1998), but it is not clear if some of these variations are due to uncertainties in estimating the velocities or some local influence like the presence of active regions.

Since the large scale flows, like the differential rotation and meridional flows are expected to play an important role in the functioning of the solar dynamo (Choudhuri, Schussler and Dikpati 1995; Brummell, Hurlburt and Toomre 1998), one may expect some changes in these

flow patterns over the solar cycle. These variations may give us some information about how the solar dynamo operates. From the splittings of global f-modes Schou (1999) has found variations in the zonal flow pattern, which are similar to the torsional oscillations observed at the solar surface. Thus it appears that these oscillations penetrate into the deeper layers. It would thus be interesting to study possible variation in these large scale flows with solar activity and how far deep these flows extend. With the high quality data collected by Michelson Doppler Imager (MDI) on board SOHO, over the last 3 years it has been possible to study these temporal variations and in this work we attempt to study possible temporal variation in large scale flows. For simplicity, we have only considered the longitudinal averages, which contain information about the latitudinal variation in these flows. For this purpose, at each latitude we have summed the spectra obtained for different longitudes to get an average spectrum which has information on the average flow velocity at each latitude. The averaging helps us in improving the reliability of results thus allowing us to infer relatively small variations in the flow velocities. We have studied both the rotational and meridional components of the flow velocity.

2. Technique

In this work we use the data obtained by the MDI instrument to measure the flow velocities at different epochs. We use four sets of data. Set 1 is data for May/June 1996, Set 2 is for July 1996, Set 3 is for April 1997 and Set 4 is for January/February 1998. These data were taken at various phases of the current solar cycle. The data consist of three dimensional power spectra obtained from full disc Dopplergrams. The Dopplergrams were taken at a cadence of 1 minute. The area being studied was tracked at the surface rotation rate. To minimize the effect of foreshortening we have only used data for the central meridian. Each power spectrum was obtained from a time series of 1664 images covering 15° in longitude and latitude. Successive spectra are separated by 15° in heliographic longitude of the central meridian. For each longitude, we have used 15 spectra centered at latitudes ranging from 52.5°N to 52.5°S with a spacing of 7.5° in latitude.

Set 1 consists of spectra from twelve longitudes, starting from central meridian at 105° to 15° of Carrington Rotation 1909 and 360° to 300° of rotation 1910. Set 2 consists of twelve longitudes from Carrington rotation 1911, central meridian at 285° to 120°, set 3 contains eight longitudes from Carrington rotation 1921, central meridian at 120° to 15° and set 4 contains nine longitudes from Carrington rotation 1932,

central meridian at 360° to 240°. The choice of these data sets was dictated by the availability of data at the time this analysis was carried out.

To extract the flow velocities and other mode parameters from the three dimensional power spectra we fit a model with asymmetric peak profiles (Basu and Antia 1999) specified by:

$$P(k_x,k_y,\nu) = \frac{\exp(A_0+(k-k_0)A_1+A_2(\frac{k_x}{k})^2+A_3\frac{k_xk_y}{k^2})(S^2+(1+Sx)^2)}{x^2+1} + \frac{e^{B_1}}{k^3} + \frac{e^{B_2}}{k^4}, \quad (1)$$

where

$$x = \frac{\nu - ck^p - U_xk_x - U_yk_y}{w_0 + w_1(k-k_0)}, \quad (2)$$

$k^2 = k_x^2 + k_y^2$, k being the total wave number, and the 13 parameters $A_0, A_1, A_2, A_3, c, p, U_x, U_y, w_0, w_1, S, B_1$ and B_2 are determined by fitting the spectra using a maximum likelihood approach (Anderson, Duvall and Jefferies 1990). Here, k_0 is the central value of k in the fitting interval and $\exp(A_0)$ is the mean power in the ring. The coefficient A_1 accounts for the variation in power with k in the fitting interval, while A_2 and A_3 terms account for the variation of power along the ring. The term ck^p is the mean frequency, while U_xk_x and U_yk_y represent the shift in frequency due to large scale flows and the fitted values of U_x and U_y give the average flow velocity over the region covered by the power spectrum and the depth range where the corresponding mode is trapped. The mean half-width is given by w_0, while w_1 takes care of the variation in half-width with k in the fitting interval. The terms involving B_1, B_2 define the background power, which is assumed to be of the same form as that used by Patrón et al. (1997). S is a parameter that controls the asymmetry, and the form of asymmetry is the same as that prescribed by Nigam and Kosovichev (1998). The details of how the fits are obtained can be found in Basu et al. (1999) and Basu and Antia (1999).

The fitted U_x and U_y for each mode represents an average of the velocities in the x and y directions over the entire region in horizontal extent and over the vertical region where the mode is trapped. We can invert the fitted U_x (or U_y) for a set of modes to infer the variation in horizontal flow velocity u_x (or u_y) with depth. We use the Regularized Least Squares (RLS) as well as the Optimally Localized Averages (OLA) techniques for inversion as outlined by Basu et al. (1999). The results obtained by these two independent inversion techniques are compared to test the reliability of inversion results.

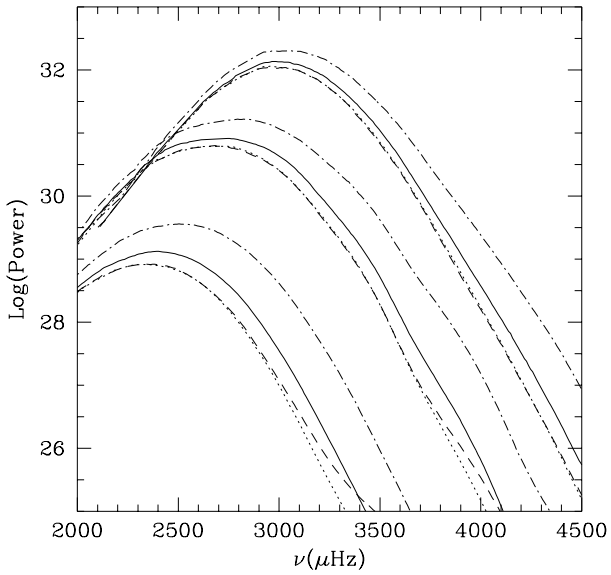

Figure 1. The power in ridges for $n = 0, 1, 2$ at different times is plotted against frequency, for region centered at the equator. The power is in arbitrary units. The continuous line is for Set 1, the dotted line for Set 2, the dashed line for Set 3 and dot-dashed line for Set 4.

3. Results

We have fitted the four sets of summed spectra to calculate various mode parameters. In this work we are mainly concerned with the variation in flow velocities with time, but it is well known that other quantities also vary with time. The variation of mean frequency with time is well-known, but it is difficult to determine this small change using ring diagram technique as the image scale is known to have changed with time to some extent. We do not find any significant variation in the width but the power in modes shows some temporal variation. Fig. 1 shows the power in $n = 0, 1, 2$ ridges in equatorial region as a function of frequency for each of the four sets of spectra. It is clear that power in Set 4, which covers a region of high activity is larger as compared to the other three sets which cover period of low activity. If this variation is real then the power in modes appears to increase with activity and the increase is quite significant at higher frequencies. Similar trend is seen in spectra centered at different latitudes. The high frequency modes which penetrate into the near surface region are more likely to be influenced by surface activity and thus a larger increase in their amplitude indicates that the driving mechanism operates in the

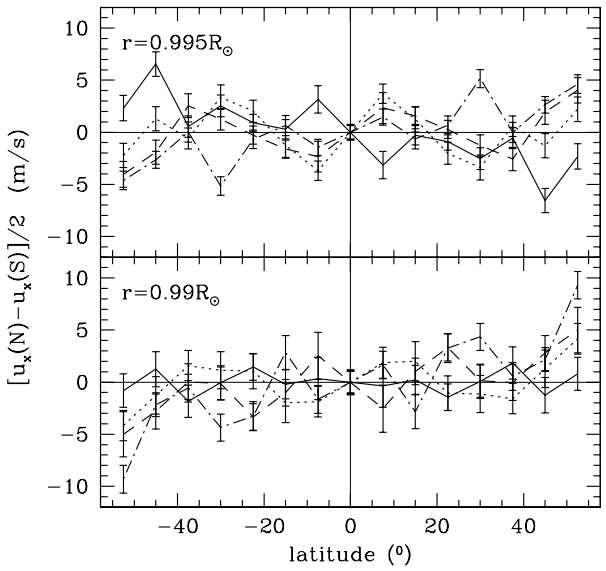

Figure 2. The north-south antisymmetric part of the rotation velocity, i.e., $[u_x(\mathrm{N}) - u_x(\mathrm{S})]/2$, plotted as a function of latitude at two different depths for all 4 sets of data. The line-types are the same as those in Fig. 1.

near surface region, where the magnetic field is known to change with activity.

3.1. The rotation velocity

The horizontal velocity u_x is known to be dominated by the rotation rate, since the area under observation is tracked only at the surface rotation rate, and the solar rotation rate is known to vary with depth. Thus the measured u_x arises from the difference in rotation rate and the tracking rate. The ring diagram technique allows us to determine the north-south antisymmetric component of rotation rate which cannot be inferred by the splittings of global modes. Fig. 2 shows the results at two different depths. There appears to be some temporal variation in this component, which is comparable to the error estimates. There is no obvious pattern in temporal variation and it is not clear if the apparent difference between different sets is not due to some systematic errors. Of course, it is possible that the antisymmetric component of the rotation velocity varies on time scales of the order of the rotation period, which is the separation between Sets 1 and 2. Such variations in the rotation rate at solar surface have been seen in Doppler measurements (Hathaway et al. 1996; Ulrich 1998).

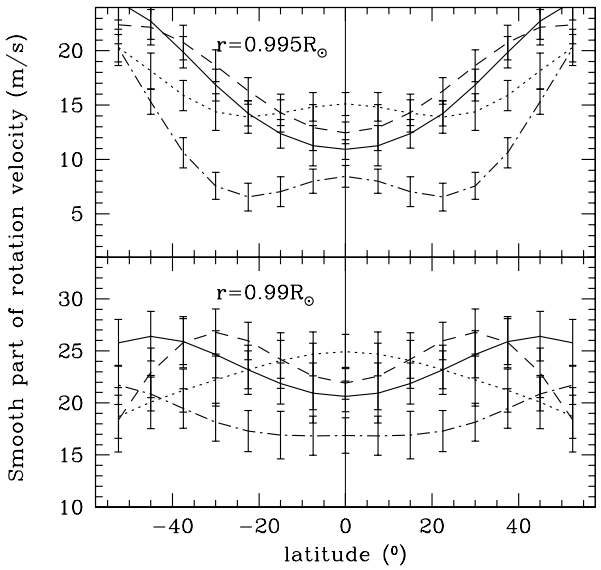

Figure 3. The smooth part of the solar rotation velocity (after subtraction of the rate at which the regions on the Sun were tracked) plotted as a function of latitude at two different depths for all 4 sets of data. The line-types are the same as those in Fig. 1.

Following Kosovichev and Schou (1997), it is possible to decompose u_x into two components, a smooth part (expressed in terms of $\cos\theta$, $\cos^3\theta$ and $\cos^5\theta$, θ being the latitude) and the remaining part, which is identified with the zonal flows. Fig. 3 shows the smooth part of the rotation rate for all 4 data sets. This result automatically has the tracking-rate which is mean rotation velocity at solar surface, subtracted. There is some variation in the rotation velocity with time. However, the change between the low activity sets (1 to 3) may not be statistically significant.

Results from global f-mode splittings show that there is a variation in the zonal flow pattern with time (Schou 1999) — the position of maximum and minimum zonal flow velocities drift equator-wards similar to the torsional oscillation pattern seen on the solar surface. Similar results have been obtained by Howe, Komm and Hill (2000) and Toomre et al. (2000) from inversion of frequency splittings. The ring diagram analysis provides a better depth resolution in near surface region as compared to the global modes and hence it can be employed to study the variation with depth in zonal flow pattern. However, it is not clear if the non-smooth part of the rotation velocity is the same as the torsional oscillations, since the latter is the time variation in rotation velocity, and there could be some variation in smooth component which would

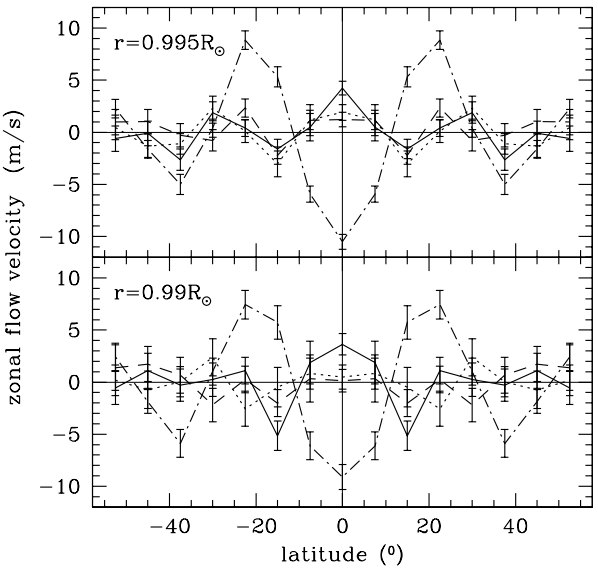

Figure 4. The zonal flow velocity plotted as a function of latitude at two different depths. The line-types are the same as those in Fig. 1.

also contribute to the torsional oscillations. This variation is in fact seen from our results in Fig. 3. Ideally, we can determine an average rotation rate over a long time period and subtract it from each measurement to get the time variation, which can possibly be identified with torsional oscillations. With only four measurements in time it is not possible to take any meaningful average and hence we attempt to identify the zonal flows with the non-smooth component as has been done by Kosovichev and Schou (1997) and Schou (1999).

It is known from earlier studies that the symmetric component of the zonal flow velocities agree well with the results from f-mode analysis (Basu et al. 1999). Fig. 4 shows the symmetric component of the zonal flow velocities for all the data sets at two different depths. Note that there is some variation in the results with time. The change is particularly significant between sets 3 and 4. Solar activity is known to have changed quite rapidly between these two epochs. The latitudinal resolution of our study is not enough to clearly judge whether the changes between results of Sets 1, 2 and 3 are statistically significant, however, there appears to be a shift towards equator in the first maxima in each hemisphere at a radial distance of $0.995R_\odot$. Results from Set 4 show the equatorial region to be rotating slower than the smoothed average rotation rate, while results from the the other sets show a faster rotation. This feature is also seen in the results obtained from f-mode splittings (Schou 1999).

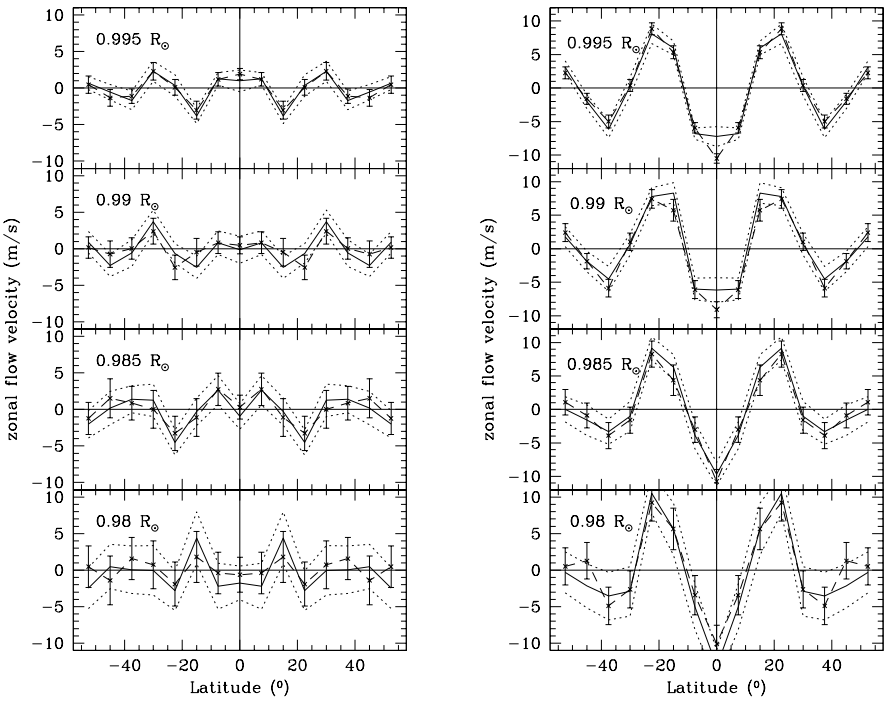

Figure 5. The zonal flow velocity plotted as a function of latitude at four different depths as marked in the figure. The panels on the left shows the result for Set 2 (low activity), while the panel on the right show the results for set 4 (high activity). In each panel, the points joined by the dashed lines are the results of an optimally localized averages (OLA) inversion. The continuous lines are the results of a regularized least squares (RLS) inversion with dotted lines showing the 1σ error limits.

To study the changes in the zonal flow pattern with depth we concentrate on Sets 2 and 4. Fig. 5 shows the zonal flow velocities for sets 2 and 4 at four different depths obtained using both RLS and OLA inversion techniques. The results obtained by the two inversion techniques agree with each other in all cases. We see that Set 4 in general has much larger flow velocities than Set 2. Furthermore, for the low activity set the direction of the flow appears to change sign as one goes deeper. This is not seen for the Set 4. However, since the overall flow velocity is small for Set 2, it is somewhat difficult to judge the significance of the change. From the results for Set 4, it appears that the zonal flow pattern persists up to a depth of at least $0.02R_\odot$ during high activity period. Because of low amplitude it is not very clear if the zonal flow pattern penetrates to the depth of $0.02R_\odot$ during the low activity period too. There may be some change in pattern with depth and it is possible that the reversal in sign of zonal flow velocity at equator occurs after

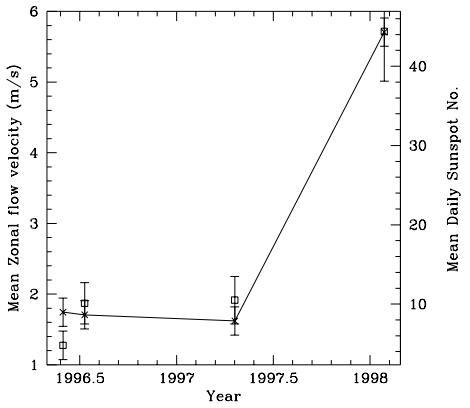

Figure 6. The average zonal flow velocity at $r = 0.995R_\odot$ plotted as a function of time (continuous line with crosses). The squares show the mean daily sunspot number during the same period when the observations were made, with the scale on the right-hand axis.

the solar minimum and starts at deeper layers, gradually advancing towards the surface, i.e., the reversal occurs earlier in deeper layers. Surface observations appear to show that the zonal flow patterns is not well defined during the time around the solar maximum (Ulrich 1998). Thus it would be interesting to check what happens in deeper layers as we approach the maximum of cycle 23. Fig. 6 shows the magnitude of zonal flow velocity averaged over all latitudes included in this study, at a depth of $0.005R_\odot$, plotted together with the mean daily sunspot number. Although we have a very small sample, it appears that the mean flow velocity increases with increase in solar activity. Similar results can be obtained from study of global modes, for which data is available for larger duration, spanning a wider range of activity level.

3.2. The meridional flow

The velocity component u_y is the meridional flow. Earlier results have shown that the predominant flow pattern at the surface is from the equator to the two poles (Giles et al. 1997; Basu et al. 1999; Braun and Fan 1998). Fig. 7 shows the meridional flow velocity for the 4 sets at two different depths. It is clear that once again the Set 4 pattern is significantly different than the others, and in particular the amplitudes of high order component appears to be larger giving rise to some oscillations over the smooth pattern.

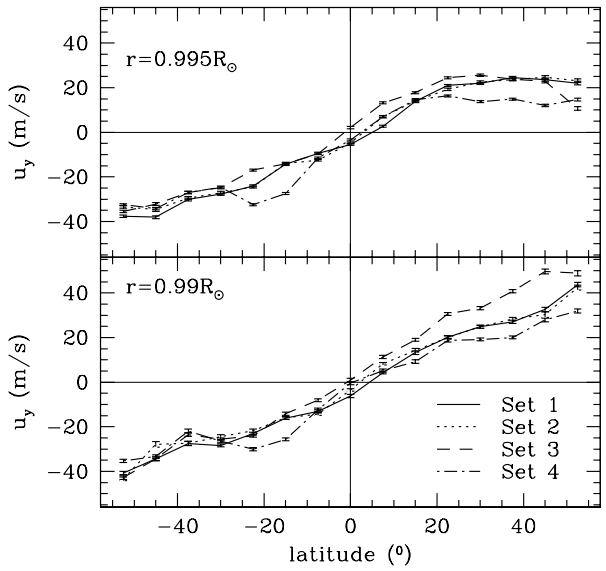

Figure 7. The meridional flow velocities obtained from the 4 data sets plotted as a function of latitude at two different depths marked in the figure. The line types are the same as those in Fig. 1.

To take a more detailed look at the time variation, following Hathaway et al. (1996) we try to express the meridional component as

$$u_y(r,\phi) = -\sum_i a_i(r) P_i^1(\cos(\phi)) \tag{3}$$

where ϕ is the colatitude, and $P_i^1(x)$ are associated Legendre polynomials. The first six terms in this expansion are found to be significant and their amplitudes are shown in Fig. 8. The component a_6 seems to show the most significant changes in the outer layers where the inversions are most reliable. The amplitude of a_6 around the depth of $0.005R_\odot$ appears to increase with solar activity and may be correlated to the mean daily sunspot number. The amplitude of the dominant component, a_2 appears to have decreased slightly during the high activity period at depths around $0.005R_\odot$. The odd terms in the expansion, which represent the north-south symmetric component of meridional flow, show much larger variation, particularly the first term $a_1(r)$. The amplitude $a_1(r)$ of the first component appears to have reduced by about 5 m/s in Set 4 as compared to Sets 1–3. In deeper layers the odd components of meridional flow appears to vary anomalously for Set 3. It is not clear if these variations in the odd components are due to instrumental effects arising from change in pointing errors, some systematic error in our analysis process, or whether they represent real changes in the

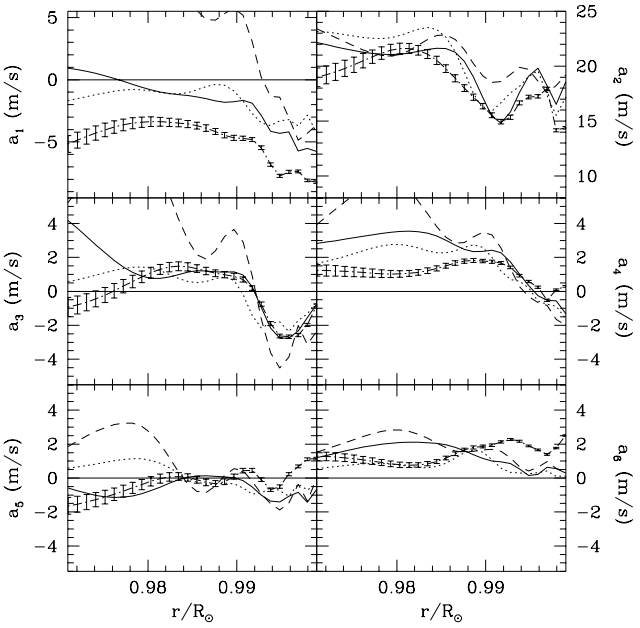

Figure 8. The amplitude of different components of the meridional flows as defined in Eq. (3). The line types are the same as those in Fig. 1. Only one set of error-bars have been shown for the sake of clarity.

subsurface flows with activity. Surface observations of meridional flows also reveal short term variations in the various components (Hathaway et al. 1996) which may correspond to some of the changes in the odd components. More detailed study involving larger number of data sets in time would be required to understand these variations.

4. Conclusions

We find that the large-scale flows in the upper part of the solar convection zone vary with time. We find that the amplitude of the zonal flow increases with increase in solar activity and besides there is some shift in the zonal flow pattern with time, which is similar to the torsional oscillations observed at the solar surface. The zonal flow pattern appears to persist up to a depth of at least $0.02R_\odot$ during period of high activity, when the amplitude is large enough for a reliable determination of the flow pattern. During the low activity period it is not clear if the zonal flow pattern penetrates to these depths. It may be noted that from the analysis of splittings of global modes Howe et al. (2000) and

Toomre et al. (2000) find that the zonal flow pattern persists to greater depths. Further, it is found that during high activity period in 1998 the equatorial region was rotating slower than the smoothed average rotation rate. It was rotating faster at other times. There is probably some depth dependence of the flow pattern during the low activity period, but its significance is not clear because of the low amplitude of the flows.

The meridional component of the flows also changes with time. If the meridional flow velocities are decomposed on a basis of associated Legendre polynomials, the high order anti-symmetric component corresponding to $P_6^1(\cos\phi)$ shows an increase in amplitude with solar activity. There are also significant changes in the symmetric component of meridional flow, but it is not clear if this is not an instrumental effect or due to some systematic errors in analysis.

Acknowledgements

This work utilizes data from the Solar Oscillations Investigation / Michelson Doppler Imager (SOI/MDI) on the Solar and Heliospheric Observatory (SOHO). SOHO is a project of international cooperation between ESA and NASA. The authors would like to thank the SOI Science Support Center and the SOI Ring Diagrams Team for assistance in data processing. The data-processing modules used were developed by Luiz A. Discher de Sa and Rick Bogart, with contributions from Irene González Hernández and Peter Giles.

References

Anderson, E. R., Duvall, T. L., Jr., and Jefferies, S. M.: 1990, *Astrophys. J.* **364**, 699.

Basu, S., and Antia, H. M.: 1999, *Astrophys. J.*, in press (astro-ph/9906252).

Basu, S., Antia, H. M., and Tripathy, S. C.: 1999, *Astrophys. J.* **512**, 458.

Braun, D. C., and Fan, Y.: 1998, *Astrophys. J.* **508**, L105.

Brummell, N. H., Hurlburt, N. E., and Toomre, J.: 1998, *Astrophys. J.* **493**, 955.

Choudhuri, A. R., Schussler, M., and Dikpati, M.: 1995, *Astron. Astrophys.* **303**, L29.

Giles, P. M., Duvall, T. L. Jr., Scherrer, P. H., and Bogart, R. S.: 1997, *Nature* **390**, 52.

González Hernández, I., Partón, J., Bogart R. S., and the SOI Ring Diagrams team: 1999, *Astrophys. J.* **510**, L153.

Hathaway, D. H., Gilman, P. A., Harvey, J. W. et al.: 1996, *Science* **272**, 1306.

Hill, F.: 1988, *Astrophys. J.* **333**, 996.

Howe, R., Komm, R., and Hill, F.: 2000, *Solar Phys.*

Kosovichev, A. G., and Schou, J.: 1997, *Astrophys. J.* **482**, L207.
Nigam, R., and Kosovichev, A. G.: 1998, *Astrophys. J.* **505**, L51.
Patrón, J., González Hernández, I., Chou, D.-Y., et al.: 1997, *Astrophys. J.* **485**, 869.
Patrón, J., González Hernández, I., Chou, D.-Y., et al.: 1998, *Astrophys. J.* **506**, 450.
Schou, J.: 1999, *Astrophys. J.*, **523**, L181
Schou, J., and Bogart, R. S.: 1998, *Astrophys. J.* **504**, L131.
Toomre, J., Christensen-Dalsgaard, J., Howe, R., Larsen, R. M., Schou, J., Thompson, M. J.: 2000, *Solar Phys.*
Ulrich, R. K.: 1998, *IAU Symp. 185*, 59.